

Mutual Slowing-Down Effects in Mixture Diffusion in Zeolites

Rajamani Krishna* and Jasper M. van Baten

Van't Hoff Institute for Molecular Sciences,
University of Amsterdam, Science Park 904,
1098 XH Amsterdam, The Netherlands

Received: June 7, 2010

Kuhn et al.¹ have used a combination of molecular simulations and experimental data to analyze the permeation characteristics of water–methanol and water–ethanol mixtures across a DDR membrane. DDR zeolite consists of cages separated by windows of $3.6 \times 4.4 \text{ \AA}$ size. The results presented in their Figure 12 deserves more detailed attention and comment. It shows the influence of mixture composition on the self-diffusivities, $D_{i,\text{self}}$, of water, methanol, and ethanol in water–methanol and water–ethanol binary mixtures determined from molecular dynamics (MD) and transition state theory (TST). With increasing alcohols concentration, the water diffusivities in both binary mixtures are reduced significantly. With increasing water concentration, the diffusivity of methanol is also reduced below the pure component value.

In a different investigation, Hasegawa et al.² have published experimental pervaporation data for water–ethanol mixtures across a CHA membrane. CHA zeolite consists of cages separated by windows of $3.8 \times 4.2 \text{ \AA}$ size. In Figure 3 of this paper it is observed that both water and ethanol permeation fluxes are reduced significantly with increased addition of partner species.

The primary objective of this note is to show that Figure 12 of Kuhn et al.¹ and Figure 3 of Hasegawa et al.² are both demonstrations of the mutual slowing-down effects for water–alcohol mixture diffusion and that this is a generic characteristic for a wide range of microporous materials.

We begin by demonstrating the mutual slowing-down effects in CHA, and produce results that are parallel to that of DDR, presented in Figure 12 of Kuhn et al.¹ The force fields used and simulation details are provided in the Supporting Information accompanying this publication. For a constant total loading of 2 molecules per cage, the self-diffusivity data, normalized with respect to the corresponding pure component values are presented in Figure 1a. The data indicate mutual slowing down for water–methanol mixture diffusion. Also, the reduction in the water diffusivity is much more significant, by 1 order of magnitude, than that for methanol. The data presented in Figure 1a provide a rationale for water–alcohol pervaporation data of Hasegawa et al.,² validating mutual slowing-down effects.

A different manner of emphasizing the mutual slowing-down effect is to compare the self-diffusivities in an equimolar mixture of water and methanol with the corresponding pure component values, determined at the same mixture occupancy

$$\theta_t = \theta_1 + \theta_2 = \Theta_1/\Theta_{1,\text{sat}} + \Theta_2/\Theta_{2,\text{sat}} = c_1/c_{1,\text{sat}} + c_2/c_{2,\text{sat}} \quad (1)$$

* Corresponding author. Tel: +31 20 6270990. Fax: +31 20 5255604. E-mail: r.krishna@uva.nl.

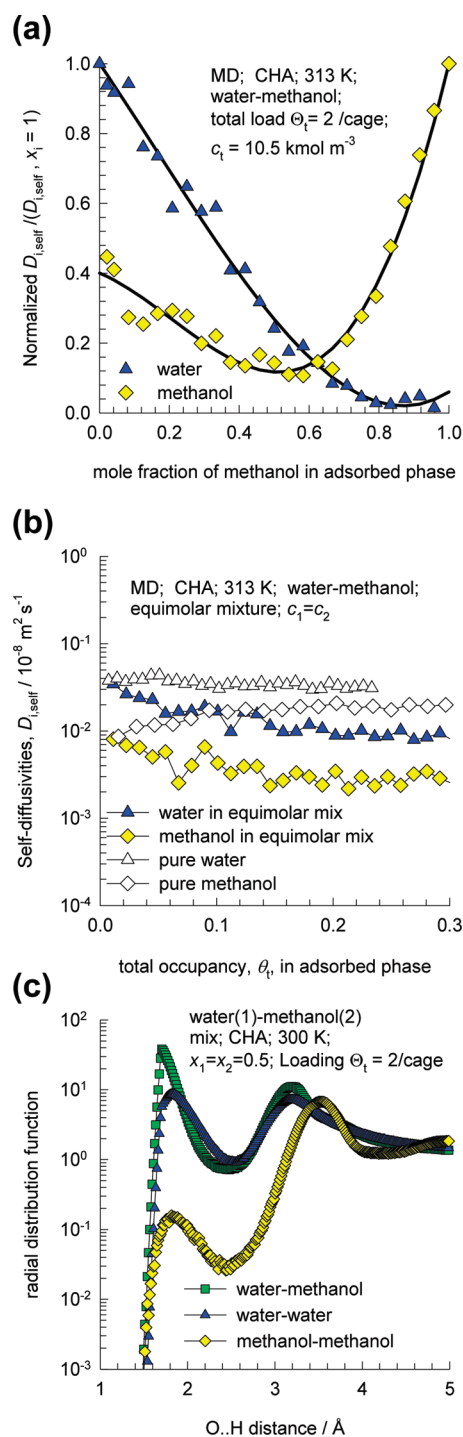


Figure 1. (a) Self-diffusivities, $D_{i,\text{self}}$, normalized with respect to the corresponding pure component value ($x_i = 1$) in water–methanol mixtures of varying composition in CHA zeolite at 313 K, and constant total mixture loading $\Theta_t = 2$ molecules per cage, corresponding to $c_1 = 10.5 \text{ kmol m}^{-3}$. (b) Self-diffusivities, $D_{i,\text{self}}$, in water–methanol equimolar mixtures ($c_1 = c_2$) in CHA zeolite at 313 K as a function of the total mixture occupancy. The total occupancy is determined using the saturation capacities $c_{i,\text{sat}} = 60$ and 28 for water and methanol respectively. (c) Radial distribution functions (RDFs) for an equimolar binary mixture of water and methanol in CHA at 313 K at a total loading of 2 molecules per cage.

The data in Figure 1b show that the self-diffusivities in the mixture are significantly lower than the corresponding values

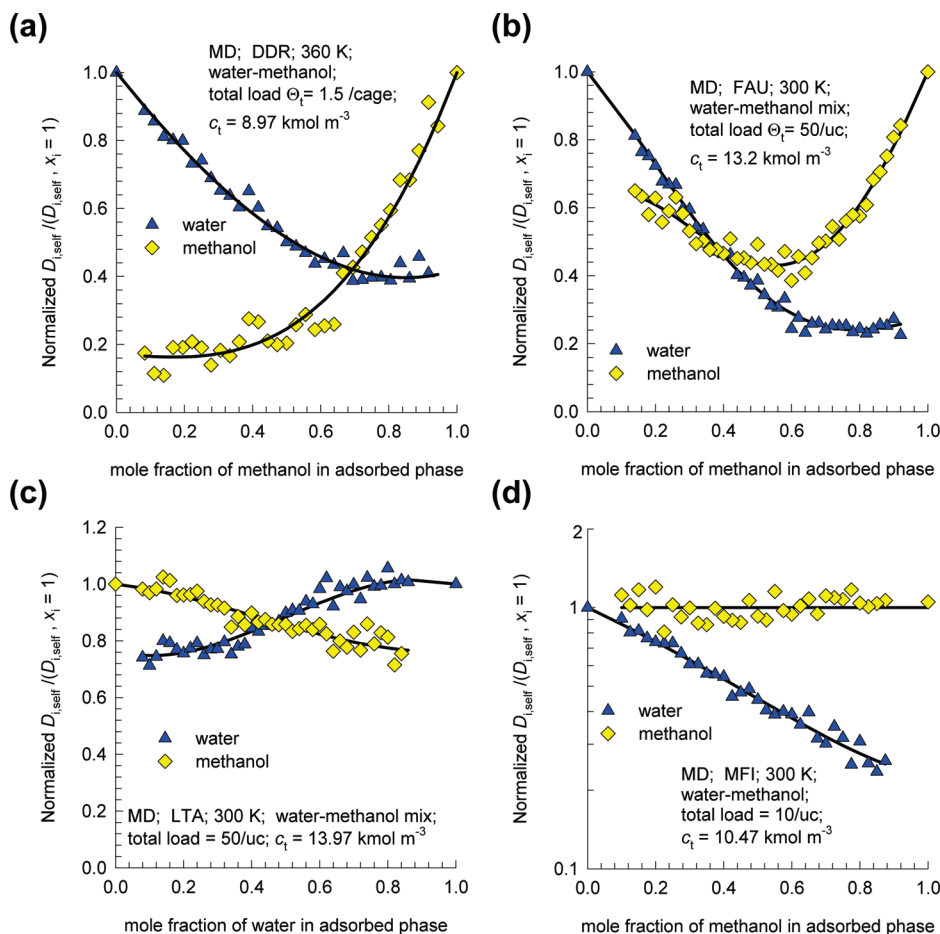


Figure 2. Self-diffusivities, $D_{i,self}$, normalized with respect to the corresponding pure component value ($x_i = 1$) in water–methanol mixtures of varying composition in (a) DDR, (b) FAU, (c) LTA, and (d) MFI zeolite at constant total mixture loading.

for the pure components for occupancies $\theta_i > 0.05$. Put another way, mutual slowing-down effects are likely to be of importance for mixture diffusion at finite occupancies.

In recent work³ we had analyzed water–alcohol diffusion in LTA, DDR, MFI, and FAU zeolites and concluded that the root cause for the mutual slowing down can be traced to much stronger hydrogen bonding between water and alcohol molecular pairs than for water–water and alcohol–alcohol pairs. The same situation holds for CHA zeolite. For an equimolar mixture of water and methanol in CHA, the radial distribution function (RDF) data for distances between O and H atoms provides confirmation of this conclusion; see Figure 1c. The first peaks occur at a separation distance of 2 Å, that is characteristic of hydrogen bonding. The first-peak height for water–methanol pairs is significantly higher than that for other molecular pairs, signifying much stronger hydrogen bonding between water and methanol than for the other two molecule–molecule pairs, as also concluded earlier for LTA, DDR, MFI, and FAU.³

The corresponding self-diffusivity data for water–methanol mixtures in DDR, FAU, and LTA zeolites as a function of the adsorbed phase methanol composition is presented in Figure 2a–c, respectively. These data are parallel to those presented for CHA in Figure 1a, and also point to mutual slowing-down in water–methanol mixture diffusion. The data for MFI zeolite in Figure 2d has a slightly different character due to strong correlations within the intersecting intersecting channel structure. The self-diffusivity of methanol is practically unaffected by water; the NMR experiments of Caro et al.⁴ provide direct experimental verification of this trend.

For water–ethanol mixtures, a similar mutual slowing-down effect manifests, as is illustrated for FAU zeolite in Figure 3a. For binary mixtures of methanol and ethanol, the more mobile methanol is slowed-down and the tardier species ethanol is speeded-up, yielding the “normal” behavior as characterized by the data for FAU zeolite in Figure 3b. For methanol–ethanol mixtures all three molecular pairs have similar degrees of hydrogen bonding and therefore there is no mutual slowing-down effect.⁵

From a close examination of the video animations accompanying our previous publication,³ it appears that hydrogen bonding between water and alcohol molecule pairs serves to act as a “flexible leash” linking the motion of the more mobile (water) and tardier (alcohol) species. The net result is that the motion of both species is retarded because the motion of an effectively larger agglomerate is to be reckoned with. During the passage of the agglomerate across the 8-ring windows of CHA, DDR, and LTA it is possible that the hydrogen bonds are first broken and then reformed once the window is crossed.

Mutual slowing-down effects, most likely caused by hydrogen bonding,⁶ are also observed for permeation of acetone–methanol mixtures across an MFI membrane.^{7,8}

For transport across a Nafion membrane in methanol fuel cell applications, strong hydrogen bonding between water and methanol is also evidenced in the molecular simulation study of Chen et al.,⁹ causing mutual slowing-down in the mixture. The NMR spectroscopy data of Hallberg et al.¹⁰ on self-diffusivities in water–methanol mixtures across a Nafion

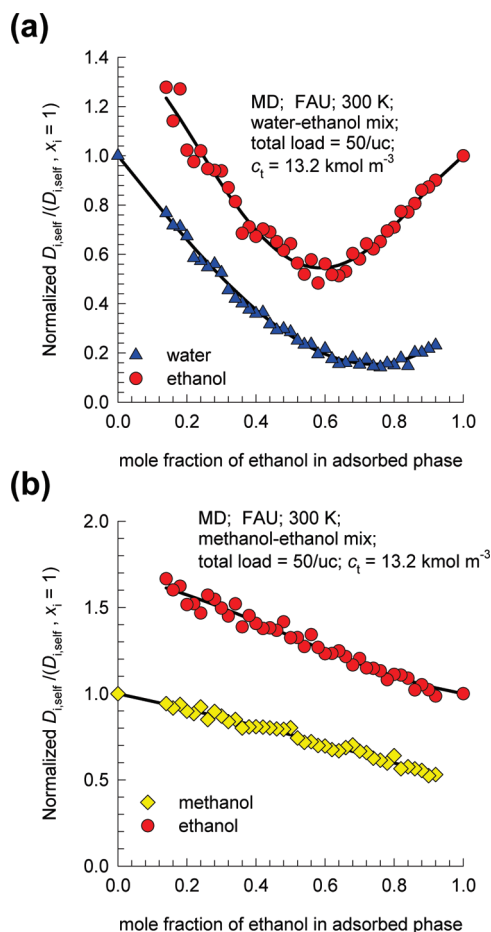


Figure 3. Self-diffusivities, $D_{i,\text{self}}$, normalized with respect to the corresponding pure component value ($x_i = 1$) in (a) water–ethanol, and (b) methanol–ethanol mixtures in FAU zeolite at 300 K and constant total mixture loading $\Theta_t = 50$ molecules per unit, corresponding to $c_t = 13.2 \text{ kmol m}^{-3}$.

membrane provides direct experimental evidence of mutual slowing-down effects.

For water–alcohols diffusion, the foregoing evidence implies that the Maxwell–Stefan diffusivities \mathfrak{D}_i in the mixture cannot be identified with the pure component value; the values in the mixture must be expected to be significantly lower.^{3,5} Additionally, the influence of mixture composition on the \mathfrak{D}_i , need to be accounted for. Furthermore, the strong hydrogen-bonding between water and alcohol causes the break down of the Vignes interpolation formula^{11,12} for estimation of correlation effects in mixture diffusion.^{3,5} These aforementioned influences have been commonly ignored in the published Maxwell–Stefan model implementations for mixture transport in water–alcohols pervaporation across DDR,¹ LTA,¹³ MFI,⁸ and methylated silica^{14,15} membranes. The published Maxwell–Stefan descriptions of transport in methanol fuel cells also ignore slowing-down effects.^{16,17}

There is a need for improved Maxwell–Stefan descriptions of water–alcohols diffusion in microporous materials, that account of mutual slowing-down effects.

Acknowledgment. R.K. acknowledges the grant of a TOP subsidy from The Netherlands Foundation for Fundamental Research (NWO–CW) for intensification of reactors. Email exchanges with F. Kapteijn were also helpful in preparation of this Comment.

Supporting Information Available: Details of the MD simulation methodologies, details of the microporous structures (unit cell dimensions, accessible pore volume), pore landscapes, description of the force fields used, and simulation data on diffusivities. This material is available free of charge via the Internet at <http://pubs.acs.org>.

Abbreviations.

Notation

c_i	concentration of species i , mol m^{-3}
$c_{i,\text{sat}}$	saturation capacity of species i , mol m^{-3}
c_t	total concentration in mixture, mol m^{-3}
$D_{i,\text{self}}$	self-diffusivity of species i , $\text{m}^2 \text{ s}^{-1}$
\mathfrak{D}_i	Maxwell–Stefan diffusivity, $\text{m}^2 \text{ s}^{-1}$
x_i	mole fraction of species i based on loading within pore, dimensionless

Greek letters

θ_i	fractional occupancy of species i , dimensionless
Θ_i	loading of i , molecules per cage or per unit cell
$\Theta_{i,\text{sat}}$	saturation capacity of i , molecules per cage or per unit cell

References and Notes

- (1) Kuhn, J.; Castillo-Sanchez, J. M.; Gascon, J.; Calero, S.; Dubbel-dam, D.; Vlugt, T. J. H.; Kapteijn, F.; Gross, J. *J. Phys. Chem. C* **2009**, *113*, 14290–14301.
- (2) Hasegawa, Y.; Hotta, H.; Sato, K.; Nagase, T.; Mizukami, F. *J. Membr. Sci.* **2010**, *347*, 193–196.
- (3) Krishna, R.; van Baten, J. M. *Langmuir* **2010**, *26*, 10854–10867.
- (4) Caro, J.; Bülow, M.; Richter-Mendau, J.; Kärger, J.; Hunger, M.; Freude, D. *J. Chem. Soc., Faraday Trans.* **1987**, *83*, 1843–1849.
- (5) Krishna, R.; Van Baten, J. M. *J. Membr. Sci.* **2010**, *360*, 476–482.
- (6) Jia, Y.; Guo, X. *Chinese J. Chem. Eng.* **2006**, *14*, 413–418.
- (7) Bowen, T. C.; Wyss, J. C.; Noble, R. D.; Falconer, J. L. *Ind. Eng. Chem. Res.* **2004**, *43*, 2598–2601.
- (8) Yu, M.; Falconer, J. L.; Noble, R. D.; Krishna, R. *J. Membr. Sci.* **2007**, *293*, 167–173.
- (9) Chen, P. Y.; Chiu, C. P.; Hong, C. W. *J. Electrochem. Soc.* **2008**, *155*, B1255–B1263.
- (10) Hallberg, F.; Vernersson, T.; Pettersson, E. T.; Dvinskikh, S. V.; Lindbergh, G.; Furó, I. *Electrochim. Acta* **2010**, *55*, 3542–3549.
- (11) Vignes, A. *Ind. Eng. Chem. Fundam.* **1966**, *5*, 189–199.
- (12) Krishna, R. *J. Phys. Chem. C* **2009**, *113*, 19756–19781.
- (13) Pera-Titus, M.; Fité, C.; Sebastián, V.; Lorente, E.; Llorens, J.; Cunill, F. *Ind. Eng. Chem. Res.* **2008**, *47*, 3213–3224.
- (14) Bettens, B.; Verhoef, A.; van Veen, H. M.; Vandecasteele, C.; Degève, J.; van der Bruggen, B. *Comput. Chem. Eng.* **2010**, *10.1016/j.compchemeng.2010.03.014*.
- (15) de Bruijn, F.; Gross, J.; Olujić, Z.; Jansens, P.; Kapteijn, F. *Ind. Eng. Chem. Res.* **2007**, *46*, 4091–4099.
- (16) Schultz, T.; Sundmacher, K. *J. Power Sources* **2005**, *145*, 435–462.
- (17) Schultz, T.; Sundmacher, K. *J. Membr. Sci.* **2006**, *276*, 272–285.

JP105240C